

# Colloidal silver nanoparticles stabilized by a water-soluble triosmium cluster

Moawia Omer Elhag Ahmed, Weng Kee Leong \*

*Department of Chemistry, National University of Singapore, 3 Science Drive 3, Singapore 117543, Singapore*

Received 19 October 2005; received in revised form 8 November 2005; accepted 9 November 2005

Available online 19 December 2005

## Abstract

Silver nanoparticles stabilized by the water soluble triosmium cluster  $\text{Os}_3(\mu\text{-H})(\text{CO})_{10}\text{S}(\text{CH}_2)_{10}\text{COO}]\text{Na}$  were prepared by both photochemical and chemical reduction of silver nitrate. The silver nanoparticles were characterized by UV–Vis spectroscopy and high resolution TEM. The particles obtained by chemical reduction showed remarkable stability.

© 2005 Elsevier B.V. All rights reserved.

*Keywords:* Silver; Nanoparticles; Osmium; Clusters

## 1. Introduction

Engineered nanoparticles of metals have generated intense interest in recent years because of their potential applications in catalysis [1], nanoscale electronics [2], and photoluminescence and electroluminescence devices [3]. The synthesis of metal colloids has been widely used as an efficient route to produce monodispersed metal nanocrystals (NCs). The most established method involves aqueous reduction of metal salts in the presence of citrate anions [4], but other methods available include thermal decomposition of organometallic compounds [5], and photolysis [6]. Surfactants must be present during NC growth to prevent aggregation and precipitation of the NCs. Electrostatic and steric interactions combine to maintain the stability of the metallic nanoparticles in solution, and ionic surfactants are generally employed [7]. For example, organic thiols have been employed to stabilize silver and gold NCs synthesized using a two-phase reduction method [8]; other commonly used surfactants include long-chain unsaturated carboxylate acids [9], and alkylamines [10].

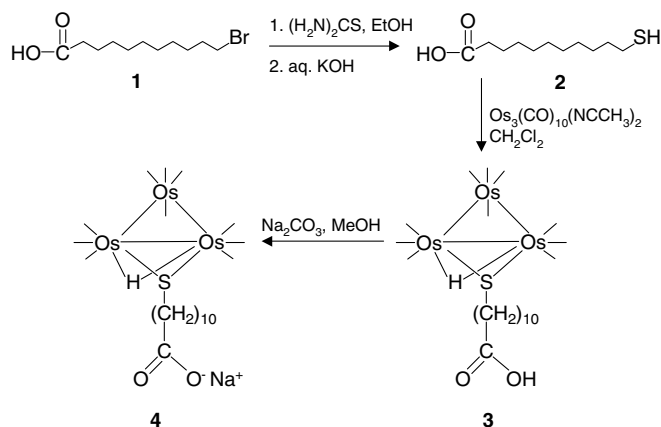
We have recently embarked on a programme to look at the anchoring of organometallic clusters onto various surfaces via different linkers as possible precursors for the generation of size-controlled metallic nanoparticles. Part of the programme was to examine the nature of such surface species, and we were interested in developing molecular or colloidal models that may allow us to better understand the surface chemistry using conventional solution spectroscopic techniques. We were thus led to examining whether we may be able to anchor an organometallic cluster onto a metallic nanoparticle. The closest known example is that of metallic nanoparticles functionalized with borane clusters [11]. We report herein our synthesis of stable colloidal silver nanoparticles stabilized with the novel water soluble organometallic surfactant  $[\text{Os}_3(\mu\text{-H})(\text{CO})_{10}\text{S}(\text{CH}_2)_{10}\text{COO}]\text{Na}$ .

## 2. Results and discussion

The synthetic route for the water soluble cluster salt  $[\text{Os}_3(\mu\text{-H})(\text{CO})_{10}\text{S}(\text{CH}_2)_{10}\text{COO}]\text{Na}$  (**4**) is outlined in Scheme 1. The steps leading from 11-bromoundecanoic acid (**1**) through the thiol derivative (**2**) to the acid complex  $\text{Os}_3(\mu\text{-H})(\text{CO})_{10}\text{S}(\text{CH}_2)_{10}\text{COOH}$  (**3**) were similar to those of published procedures [12]. Compound **3** has also been characterised by single crystal X-ray crystallography;

\* Corresponding author.

*E-mail address:* [chmlwk@nus.edu.sg](mailto:chmlwk@nus.edu.sg) (W.K. Leong).



Scheme 1.

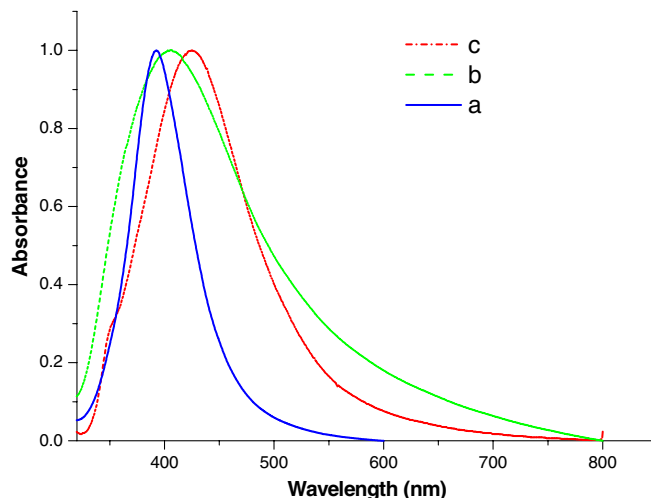
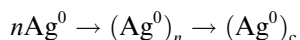
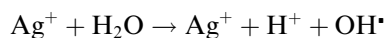


Fig. 2. UV-Vis spectra of silver nanoparticles: (a) uncapped hydrosol, (b) silver capped with **4**, obtained by chemical reduction method, and (c) capped with **4**, obtained by photochemical reduction method.

although the quality of the crystal data was poor, it was nevertheless sufficient for the gross structural features to be determined and the ORTEP plot is shown in Fig. 1.

When compound **4** was mixed with the aqueous silver nitrate solution and stirred for 12 h, the colour changed from light yellow to a yellowish-brown. The UV-Vis spectrum showed a red shift in the absorption maxima centered around 425 nm, indicating successful attachment of **4** onto the silver nanoparticles (Fig. 2c) [9]. The formation of the silver colloids has been attributed to visible light induced photooxidation of water by excited  $\text{Ag}^+$ , resulting in the formation of Ag atoms ( $\text{Ag}^0$ ),  $\text{H}^+$  and  $\text{OH}^-$ . Subsequent agglomeration of  $\text{Ag}^0$  produced silver clusters ( $\text{Ag}^0$ )<sub>n</sub> and then silver colloids ( $\text{Ag}^0$ )<sub>c</sub> which are stabilized by the water soluble surfactants such as **4** [13]



The TEM images of dried silver particles synthesized from a solution  $5 \times 10^{-3}$  M in silver nitrate and  $6.25 \times 10^{-4}$  M in **4** are shown in Fig. 3. The Ag particles have a spherical form, the particle sizes ranging over a large range although many are from 5 to 14 nm in diameter. As is clearly visible in Fig. 3b, the nanoparticles are crystalline. An EDX (energy-dispersive X-ray microanalysis) spectrum of the region imaged in Fig. 3b showed the presence of Ag (characteristic peaks at 3.10 KeV) and Os (characteristic

peaks at 2, 8, 9, 10.2 and 12 KeV) (Fig. 4), thus confirming the association of **4** with the Ag particles.

A similar yellowish-brown colloidal solution of silver was obtained using the chemical reduction method with  $\text{NaBH}_4$ . The UV-Vis spectrum (Fig. 2b) exhibits spectral features similar to those reported for silver nanoparticles dispersed in water with sodium oleate prepared by chemical reduction method [9]. The hypsochromic shift in the surface plasmon band from 390 to 408 nm provides clear evidence for the absorption of **4** onto the surface of the Ag particles. TEM images of the silver nanoparticles show that they are spherical, with diameters primarily in the 4–12 nm range (Fig. 5); this is again comparable to those generated with long chain carboxylates as stabilisers [9]. An EDX spectrum again confirmed the association of **4** with the silver particles.

There are clear differences between the nanoparticles prepared using the two methods. For instance, the particle sizes from the TEM images show that the nanoparticles obtained by the photochemical reduction method have a wider variation in sizes than those using the chemical reduction method. The UV absorption maximum in the former is also red shifted compared to that in the latter (421 and 408 nm, respectively). This may be ascribed to the formation of an insoluble brown solid of a silver salt of **4** in the photochemical reduction method; its IR spectrum is identical to that of pure **4** itself. We believe that the  $\text{Ag}^+$  salt of **4** is precipitated (which is observed as the immediate formation of a brown precipitate on mixing the solutions), onto which Ag particles deposit; a similar observation has been made in the oleate system [9a]. This leads to a poorer size distribution and larger observed particle sizes. A  $^1\text{H}$  NMR spectrum (in  $\text{D}_2\text{O}$ ) of the silver colloids generated by chemical reduction showed that the hydride signal, although broadened, was at a similar chemical shift to that observed for the free acid **3**, suggesting that the osmium cluster core does not interact significantly

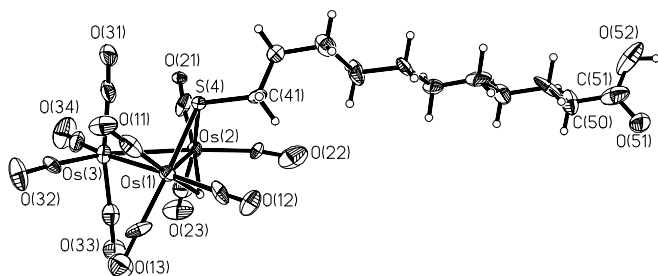


Fig. 1. ORTEP plot showing the molecular structure of compound **3**. Thermal ellipsoids are drawn at the 50% probability level.

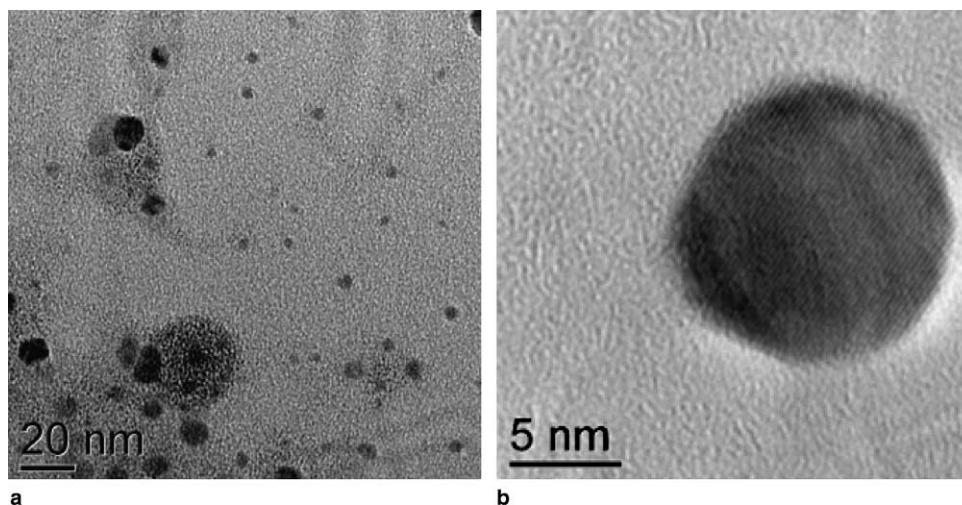


Fig. 3. TEM images of dried Ag particles stabilized with **4** prepared by the photochemical reduction method.

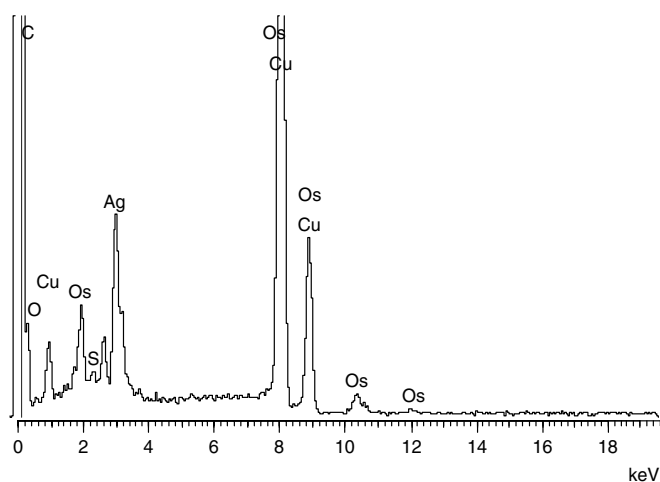


Fig. 4. An EDX spectrum obtained from the region imaged in Fig. 3b. Cu lines are from the copper grid on which the samples were deposited.

with the surface of the Ag nanoparticles. Furthermore, the IR spectrum also shows the COO symmetric and asymmetric stretching bands at  $1546$  and  $1390\text{ cm}^{-1}$ , the latter being rather broad; these are consistent with the carboxylate interacting with the silver surface and via a monodentate fashion [9].

Recently, Wei Wang and coworkers have reported that while unsaturated long chain carboxylates (e.g., oleate) are useful stabilizers in Ag nanoparticle preparation, the saturated long-chain analogues (e.g., stearate) are hardly adsorbed onto the surface of the Ag particles in an aqueous phase [9]. We found that Ag nanoparticles stabilized with a saturated long-chain carboxylate attached to a trisium cluster are more stable compared to those previously prepared with saturated long chain carboxylates, which have been reported to be stable for up to only a few days. In fact, the UV–Vis spectrum of our cluster-stabilised silver nanoparticles was found to be invariant over a three months period (Fig. 6). Furthermore, we have heated our nanopar-

ticles at temperatures up to  $100\text{ }^{\circ}\text{C}$  and for up to 1 h, and the UV–Vis spectrum suggests that they remain unchanged. It thus appears that the trisium cluster plays a role in stabilizing the Ag nanoparticles in water. One possibility is that the hydrophobic and bulky organometallic cluster may act as a steric shield, and so has a similar net effect as the rigidity imposed by the C=C bonds in unsaturated carboxylates in maintaining nanoparticle stability [9]; such an effect has also been proposed recently for a system based on tris(phenanthroline)ruthenium(II) [14].

### 3. Conclusion

We have reported a direct synthesis of dispersed silver nanoparticles by photochemical reduction in the presence of the water soluble trisium cluster **4** acting as surfactant and compared them with those generated by the most commonly used chemical reduction method employing sodium borohydride. The silver nanoparticles from the chemical reduction method showed very good stability and narrow size distribution. We are currently investigating the potential application of such systems.

### 4. Experimental

#### 4.1. General procedures

All synthetic steps up to compound **4** were carried out under an atmosphere of nitrogen using standard Schlenk techniques.  $^1\text{H}$  NMR spectra were recorded on a Bruker ACF300 NMR spectrometer as  $\text{CDCl}_3$  solutions unless otherwise stated; chemical shifts reported are referenced against the residual proton signals of the solvents. UV–Vis spectra were recorded using a SHIMADZU UV-1601 PC spectrometer. TEM images were recorded on a JEOL JEM 3010 TEM at an accelerating voltage of 300 kV. TEM samples were prepared by placing a drop of the silver colloids onto a carbon-coated Cu grid. All elemental anal-

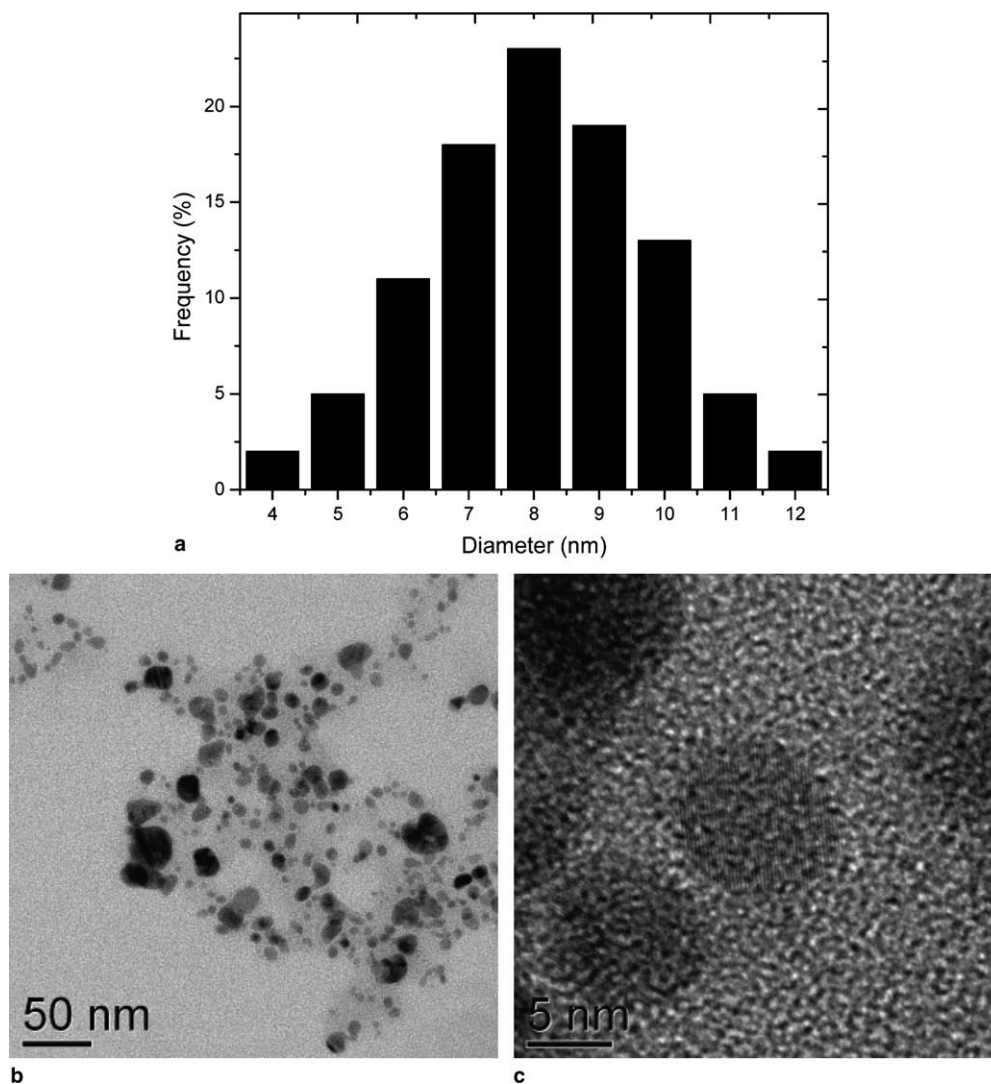


Fig. 5. TEM images of dried Ag particles stabilized with **4** prepared by the chemical reduction method.

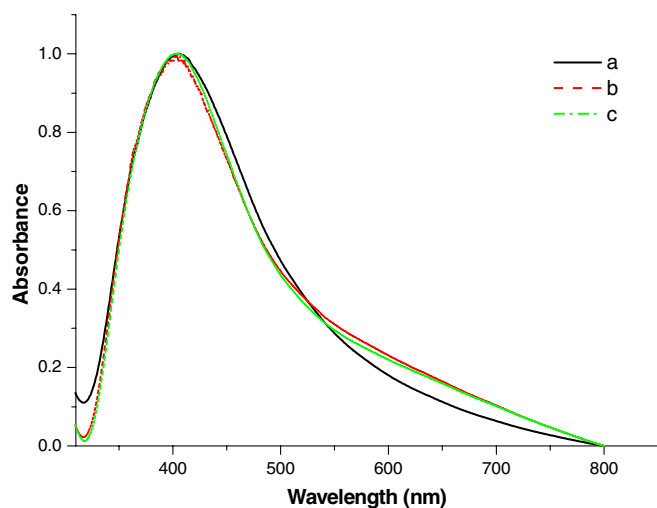


Fig. 6. UV-Vis spectrum of Ag colloids capped with **4** generated by the chemical reduction method and maintained at room temperature for (a) 1 month, (b) 2 months, and (c) 3 months.

yses were performed by the microanalytical laboratory at NUS. The cluster  $\text{Os}_3(\text{CO})_{10}(\text{NCCH}_3)_2$  was prepared according to the literature method [15], from  $\text{Os}_3(\text{CO})_{12}$  which were purchased from Oxxem Ltd. and used as supplied. All other reagents were from commercial sources and used without further purification.

#### 4.2. Synthesis of 11-mercaptoundecanoic acid (**2**)

To a stirred solution of 11-bromoundecanoic acid (**1**) (730 mg, 2.76 mmol) in ethanol (40 ml) was added thiourea (420 mg, 5.52 mmol). The reaction mixture was heated under reflux for 6 h, and the solvent was then removed under reduced pressure. The resulting solid residue was mixed with KOH (773 mg, 13.80 mmol) and deionized water (40 ml), and then refluxed for 3 h. This was then acidified with 1 M aq. HCl and then extracted with dichloromethane. The organic layer was separated, dried over  $\text{MgSO}_4$ , and the solvent was then distilled off under reduced

pressure. The residue was purified by TLC on silica gel plates (hexane/EtOAc, 3:1, v/v, as eluant) to yield a white solid. Yield = 400 mg (67%).  $^1\text{H NMR}$ :  $\delta$  1.23–1.83 (m, 16H,  $\text{CH}_2$ ), 2.51 (q, 2H,  $\text{CH}_2\text{S}$ ), 2.34 (t, 2H,  $\text{COCH}_2$ ). Anal. Calc. for  $\text{C}_{11}\text{H}_{21}\text{O}_2\text{S}$ : C, 60.79; H, 9.74; S, 14.75. Found: C, 60.51; H, 9.71; S, 14.28%. FAB-MS:  $m/z$  217.1 ( $\text{M}^+$ ).

#### 4.3. Synthesis of $\text{Os}_3(\mu\text{-H})(\text{CO})_{10}\text{S}(\text{CH}_2)_{10}\text{COOH}$ (**3**)

The cluster  $\text{Os}_3(\text{CO})_{10}(\text{NCCH}_3)_2$  (200 mg, 0.22 mmol) was stirred with **2** (48 mg, 0.22 mmol) in dichloromethane (30 ml) at room temperature for 12 h. The solvent was removed under reduced pressure and the product was purified by TLC to yield a yellow solid. Yield = 140 mg (60%). IR ( $\text{CH}_2\text{Cl}_2$ )  $\nu$  (CO): 2106 (w), 2063 (s), 2058 (w), 2018 (s), 1998 (w), 1637 (s)  $\text{cm}^{-1}$ ;  $\nu$ (CH): 2921 (m), 2857 (m)  $\text{cm}^{-1}$ .  $^1\text{H NMR}$ :  $\delta$  1.23–2.09 (m, 16H,  $\text{CH}_2$ ), 2.35 (t, 2H,  $\text{CH}_2\text{S}$ ), 3.43 (t, 2H,  $\text{COCH}_2$ ),  $-17.41$  (s, 1H, OsHOs). Anal. Calc. for  $\text{C}_{21}\text{H}_{22}\text{O}_12\text{SOs}_3$ : C, 23.59; H, 2.07; S, 3.00. Found: C, 24.05; H, 1.91; S, 2.63%. FAB-MS:  $m/z$  1069.0 ( $\text{M}^+$ ). X-ray data: triclinic,  $P\bar{1}$ ;  $a = 7.7438(9)$ ,  $b = 9.2082(10)$ ,  $c = 21.463(2)$ ,  $\alpha = 93.080(2)$ ,  $\beta = 93.103(2)$ ,  $\gamma = 113.076(2)$ ,  $V = 1401.3(3)$ ;  $Z = 2$ ,  $\rho_c = 2.534 \text{ g cm}^{-3}$ ,  $\mu = 13.699 \text{ mm}^{-1}$ ;  $F(000) = 976$ ; plate ( $0.26 \times 0.24 \times 0.06 \text{ mm}^3$ ); 7862 independent reflections out of 20883,  $R_{\text{int}} = 0.0517$ ;  $\text{GoF} = 1.197$ ,  $R_1 = 0.1229$ ,  $wR_2 = 0.3208$  for all reflections, 13 restraints and 338 parameters.

#### 4.4. Synthesis of $[\text{Os}_3(\mu\text{-H})(\text{CO})_{10}\text{S}(\text{CH}_2)_{10}\text{COO}]\text{Na}$ (**4**)

To the acid **3** (100 mg, 0.09 mmol) in methanol (20 ml) was added sodium carbonate (18.7 mg, 0.19 mmol). The mixture was refluxed for 3 h, cooled to room temperature, and then the excess sodium carbonate filtered off. The solvent was removed under reduced pressure to afford **4** obtained as yellow solid. Yield = 97 mg (95%). IR (KBr)  $\nu$ (CO): 2110 (w), 2057 (w), 2013 (s), 1934 (w), 1652(m), 1410 (m)  $\text{cm}^{-1}$ .  $^1\text{H NMR}$  ( $\text{D}_2\text{O}$ ):  $\delta$  1.31–1.87 (m, br, 16H,  $\text{CH}_2$ ), 2.17 (br, 2H,  $\text{CH}_2\text{S}$ ), 3.36 (br, 2H,  $\text{COCH}_2$ ),  $-17.4$  (s, br, 1H, OsHOs). Anal. Calc. for  $\text{C}_{21}\text{H}_{21}\text{O}_{12}\text{SNaOs}_3$ : C, 23.12; H, 1.94; S, 2.94. Found: C, 22.85; H, 1.75; S, 2.73%. FAB-MS:  $m/z$  1090.90 ( $\text{M}^+$ ).

### 5. Preparation of colloids

#### 5.1. Photochemical reduction

The silver colloids were prepared according to the literature method [16]. Typically, aqueous solutions of  $\text{AgNO}_3$  ( $5 \times 10^{-3} \text{ M}$ ) and **4** ( $6.25 \times 10^{-4} \text{ M}$ ) were mixed and then exposed to visible light, while continuously stirred, for 12 h.

#### 5.2. Chemical reduction

The procedures were essentially the same as those described by Wei Wang et al. [9]. In a typical preparation, an aqueous solution of  $\text{AgNO}_3$  (25 ml,  $5 \times 10^{-3} \text{ M}$ ) was

added into a freshly prepared aqueous solution (25 ml) containing  $\text{NaBH}_4$  ( $2 \times 10^{-2} \text{ M}$ ) and **4** ( $6.25 \times 10^{-4} \text{ M}$ ) with vigorous stirring, while cooled in an ice-water bath. A yellowish-brown colloid of silver was obtained almost immediately. The mixture was then allowed to warm to room temperature and stirring was continued for 3 h to ensure completion.

### 6. Crystal structure determination

A crystal grown by layering of a dichloromethane solution with hexane was mounted on quartz fibres. X-ray data were collected on a Bruker AXS APEX system, using  $\text{Mo K}\alpha$  radiation, at 223 K with the SMART suite of programs [17]. Data were processed and corrected for Lorentz and polarisation effects with SAINT [18], and for absorption effects with SADABS [19]. Structural solution and refinement were carried out with the SHELXTL suite of programs [20].

The structure was solved by direct methods to locate the Os and S atoms, followed by difference maps for the light, non-hydrogen atoms. All non-hydrogen atoms were generally given anisotropic displacement parameters in the final model. The data quality was poor and there appeared to be disorder of the sulphur atom; this was modeled with two sites, one on either side of the  $\text{Os}_3$  plane. The occupancies for the two sites were allowed to refine but constrained to sum to unity, and both sites were given the same set of anisotropic thermal parameters. Vibration restraints were placed on one carbonyl and two of the O atoms also had to be restrained to have isotropic thermal motion to keep the refinement reasonable.

### Acknowledgement

This work was supported by an A\*STAR grant (Research Grant No. 022 109 0061).

### Appendix A. Supplementary data

Experimental and refinement details for the crystallographic studies, tables of crystal data and structure refinement, atomic coordinates, isotropic and anisotropic thermal parameters, complete bond parameters, and hydrogen coordinates (10 pages). Crystallographic data in CIF format. Ordering information is given on any current masthead page. Supplementary data associated with this article can be found, in the online version, at doi:10.1016/j.jorganchem.2005.11.015.

### References

- [1] (a) G. Schmid, V. Maihack, F. Lantermann, S. Peschel, J. Chem. Soc., Dalton Trans. (1996) 589; (b) H. Ohde, C.M. Wai, J. Kim, M. Ohde, J. Am. Chem. Soc. 124 (2002) 4540; (c) T. Sun, K. Seff, Chem. Rev. 94 (1994) 857; (d) X.E. Verykios, F.P. Stein, R.W. Coughlin, Catal. Rev. Sci. Eng. 22 (1980) 197.

- [2] (a) D.L. Klein, R. Roth, A.K.L. Lim, A.P. Alivisatos, P.L. McEuen, *Nature* 389 (1997) 699;  
(b) L.N. Lewis, *Chem. Rev.* 93 (1993) 2693;  
(c) A.P. Alivisatos, *Science* 271 (1996) 933;  
(d) D.I. Gittins, D. Bethell, D.J. Schiffrin, R.J. Nichols, *Nature* 408 (2000) 67.
- [3] K.L. Kelly, E. Coronado, L.L. Zhao, G.C. Schatz, *J. Phys. Chem. B* 107 (2003) 668.
- [4] J. Turkevich, P.C. Stevenson, J. Hillier, *Disc. Faraday Soc.* 11 (1951) 55.
- [5] S. Sun, C.B. Murray, *J. Appl. Phys.* 85 (1999) 4325.
- [6] W. Wang, S.A. Asher, *J. Am. Chem. Soc.* 123 (2001) 12528.
- [7] Y. Lin, R.G. Finke, *J. Am. Chem. Soc.* 116 (1994) 8335.
- [8] M. Brust, J. Fink, D. Bethell, D.J. Schiffrin, C.J. Kiely, *J. Chem. Soc., Chem. Commun.* (1995) 1655.
- [9] (a) W. Wang, S. Efrima, O. Regev, *Langmuir* 14 (1998) 602;  
(b) W. Wang, X. Chen, S. Efrima, *J. Phys. Chem. B* 103 (1999) 724.
- [10] S.D. Bunge, T.J. Boyle, T.J. Headley, *Nano Lett.* 3 (2003) 901.
- [11] G. Schmid, R. Pugin, W. Meyer-Zaika, U. Simon, *Eur. J. Inorg. Chem.* (1999) 2051.
- [12] (a) S. Flink, B.A. Boukamp, A. van den Berg, F.C.J.M. van Veggel, D.N. Reinhoudt, *J. Am. Chem. Soc.* 120 (1998) 4652;  
(b) E.W. Ainscough, A.M. Brode, R.K. Coll, B.A. Coombridge, J.M. Waters, *J. Organomet. Chem.* 556 (1998) 197.
- [13] K. Sudhir, *Langmuir* 14 (1998) 1021.
- [14] C.R. Mayer, E. Dumas, F. Sécheresse, *J. Chem. Soc., Chem. Commun.* (2005) 345.
- [15] J.N. Nicholls, M.D. Vargas, *Inorg. Synth.* 28 (1989) 234.
- [16] J. Gao, J. Fu, C. Lin, J. Lin, Y. Han, X. Yu, C. Pan, *Langmuir* 20 (2004) 9775.
- [17] SMART Version 5.628, Bruker AXS Inc., Madison, WI, USA, 2001.
- [18] SAINT+ Version 6.22a, Bruker AXS Inc., Madison, WI, USA, 2001.
- [19] G.M. Sheldrick, *SADABS*, 1996.
- [20] SHELXTL version 5.03, Siemens Energy & Automation Inc., Madison, WI, USA.